

See discussions, stats, and author profiles for this publication at: <https://www.researchgate.net/publication/8972418>

# Girard-Egrot A, Chauvet J-P, Gillet G, Moradi-Améli M.. Specific interaction of the antiapoptotic protein Nr-13 with phospholipid monolayers is prevented by the BH3 domain of Bax....

ARTICLE *in* JOURNAL OF MOLECULAR BIOLOGY · FEBRUARY 2004

Impact Factor: 4.33 · DOI: 10.1016/j.jmb.2003.10.028 · Source: PubMed

---

CITATIONS

19

---

READS

10

## 4 AUTHORS, INCLUDING:



Germain Gillet

Cancer Research Center of Lyon

68 PUBLICATIONS 900 CITATIONS

SEE PROFILE



Mahnaz Moradi-Améli

Claude Bernard University Lyon 1

26 PUBLICATIONS 398 CITATIONS

SEE PROFILE

# Specific Interaction of the Antiapoptotic Protein Nr-13 with Phospholipid Monolayers is Prevented by the BH3 Domain of Bax

The paper is dedicated to the memory of Professor J. P. Chauvet

**Agnès Girard-Egrot<sup>1</sup>, Jean-Paul Chauvet<sup>2†</sup>, Germain Gillet<sup>3\*‡</sup> and Mahnaz Moradi-Améli<sup>3\*‡</sup>**

<sup>1</sup>Laboratoire de Génie  
Enzymatique et Biomoléculaire  
CNRS-UCBL UMR 5013  
43, Bd du 11 Novembre 1918  
69622 Villeurbanne cedex  
France

<sup>2</sup>Ingénierie et Fonctionnalisation  
des Surfaces, CNRS-ECL UMR  
5621, 36, Av. Guy de Collogne  
69134 Ecully cedex, France

<sup>3</sup>Institut de Biologie  
et Chimie des Protéines  
CNRS-UCBL UMR 5086  
7, Passage du Vercors  
69367 Lyon cedex 7, France

Members of the Bcl-2 protein family regulate apoptosis by controlling the release of apoptogenic proteins such as cytochrome *c* from the mitochondrial intermembrane space. Proapoptotic members induce release by increasing outer membrane permeability, while antiapoptotic members prevent this. The activity of Bcl-2 proteins depends mostly on their insertion into the mitochondrial membrane, which is reported to occur *via* putative channels formed by the two central hydrophobic helices. The pro- and antiapoptotic activity of Bcl-2 proteins can also be modulated by heterodimerization between antagonists through the BH3 domain of proapoptotic members, though the position of the heterodimer with respect to the membrane has never been elucidated. In this work, the membrane insertion capacity of the antiapoptotic Bcl-2 related protein Nr-13 was explored, using monolayer expansion measurements. Nr-13 penetrates into the monolayer with a molecular cross-section of 1100 Å<sup>2</sup>, thereby implicating almost all  $\alpha$ -helical domains of the molecule in this process. A mutant protein, bearing neutral instead of acidic residues in the loop between the two putative channel-forming fifth and sixth  $\alpha$ -helices, retained the ability to interact with the lipid monolayer, suggesting that the membrane insertion of Nr-13 is not exclusively  $\alpha$ 5- $\alpha$ 6-dependent. In contrast, the specific interaction of Nr-13 with the monolayer was prevented by heterodimer formation with the BH3 domain of proapoptotic Bax. These findings are discussed in terms of a model for monolayer insertion in which the antiapoptotic Nr-13 and proapoptotic proteins exert their antagonistic effects by preventing each other from reaching the membrane.

© 2003 Elsevier Ltd. All rights reserved.

\*Corresponding authors

**Keywords:** apoptosis; Bcl-2; Bax; monolayers; membrane

† Deceased.

‡ G.G. and M. Moradi-Améli contributed equally to this work.

Abbreviations used: BH, domain, Bcl-2 homology domain; CD, circular dichroism; DMPC, 1,2-dimiristoyl-*sn*-glycero-3-phosphocholine; DMPE, 1,2-dimiristoyl-*sn*-glycero-3-phosphoethanolamine; DMPG, 1,2-dimiristoyl-*sn*-glycero-3-phosphoglycerol; DPPC, 1,2-dipalmitoyl-*sn*-glycero-3-phosphocholine; DTT, dithiothreitol; LC, liquid-condensed; LE, liquid-expanded; Nr-13 $\Delta$ TM, Nr-13 devoid of its putative C terminal transmembrane domain; PC, phosphatidylcholine; PE, phosphatidylethanolamine; PG, phosphatidylglycerol; PTP, permeability transition pore; tBid, truncated Bid.

E-mail addresses of the corresponding authors: g.gillet@ibcp.fr; m.moradi@ibcp.fr

## Introduction

Proteins of the Bcl-2 family are key regulators of the apoptotic process in multicellular organisms. The cell-death regulatory activity of these molecules depends mostly on their ability to modulate the release of cytochrome *c*<sup>1,2</sup> and other apoptogenic proteins enclosed in the mitochondrial intermembrane space, including Smac/Diablo.<sup>1,3</sup> The Bcl-2 family consists of proapoptotic members (e.g. Bax, Bak, Bad, Bcl-x<sub>s</sub>, Bid, and Bim/Bod), which trigger mitochondrial protein release, and antiapoptotic members (e.g. Bcl-2, Bcl-x<sub>L</sub>, Bcl-w, Bfl-1/A1, Mcl-1, Boo/Diva, and Nr-13), which

inhibit it.<sup>4</sup> All these proteins share one to four conserved domains known as Bcl-2 homology (BH) domain (BH1–BH4). The proapoptotic proteins are subdivided into two groups: multidomain proteins such as Bax and Bak; and BH3-domain-only proteins such as Bid, Bim, and Bad. The BH3 domain functions as the death domain in the proapoptotic molecules. In addition, Bcl-2 family members possess a C terminal stretch of hydrophobic residues, predicted to be a transmembrane domain, that helps localize them to intracellular membranes, primarily the outer mitochondrial membrane.<sup>1,4</sup>

The Bcl-2 family members have a strong tendency to form homodimers as well as heterodimers. Heterodimerization between opposing anti- and proapoptotic members, which occurs *via* BH3 domain, modulates their respective activities.<sup>1,3</sup> Recently, it was demonstrated that both Bax and Bak homooligomerize as a result of apoptotic stimuli to form a complex in the mitochondrial membrane that leads to disruption of mitochondrial integrity and apoptosis. This oligomerization process seems to be promoted by BH3-only proteins,<sup>5–7</sup> although it was shown very recently that truncated Bid (tBid) also homooligomerizes, and disrupts mitochondrial membranes.<sup>8</sup> The antiapoptotic members of the Bcl-2 family, such as Bcl-2 or Bcl-x<sub>L</sub>, prevent oligomerization by interacting with Bax or Bak, or by sequestering BH3-only proteins and preventing them from promoting Bax or Bak oligomerization.<sup>1,7,9</sup> The nature of the spatial interaction of Bax with antiapoptotic members at the level of the mitochondrial membrane has not, however, been demonstrated.

Current models propose that Bcl-2 proteins exert their function either by forming pores in mitochondrial membranes themselves,<sup>10–12</sup> or by modulating endogenous mitochondrial channels through protein–protein interactions.<sup>5,13,14</sup> The pore-forming function was first proposed based on the structural similarity of Bcl-x<sub>L</sub> and the pore-forming domains of bacterial toxins such as diphtheria toxin and colicins.<sup>15</sup> The three-dimensional structures of Bid, Bax, and Bcl-2 show similar structural features,<sup>16</sup> with a bundle of six to seven  $\alpha$  helices including two central hydrophobic helices forming the core of the molecule. These central helices may constitute the potential to form channels in the membrane.<sup>10,17</sup> Subsequently, several laboratories have attempted to reproduce this function using either lipid vesicles or planar membranes.<sup>11,12,18–21</sup> Nonetheless, the regulation of mitochondrial outer membrane permeability is still controversial. The tendency of the proapoptotic Bcl-2 members to oligomerise at the outer mitochondrial membrane, together with their capacity to induce protein release from the intermembrane space, suggest a “pore-forming model”, consistent with the fact that Bax induces transport of cytochrome *c* in liposomes.<sup>11</sup> In contrast, regarding the function of antiapoptotic members in the prevention of Bak or Bax oligomerization,<sup>7,9</sup> or in the maintenance of

mitochondrial integrity,<sup>1–4</sup> such a model might be irrelevant for such functions. Elucidating the behavior of antiapoptotic protein in the membrane will, therefore, be a crucial step towards understanding the mechanism of apoptosis regulation. With this aim, we have used Langmuir film balance technology, based on phospholipid displacement in monolayers, to study lipid–protein interactions. Monomolecular films are attractive investigative models, since the thermodynamic relationship between monolayer and bilayer membranes is direct, and also, at the air–water interface monolayers overcome the limitation of lipid lateral-packing regulation encountered in bilayers.<sup>22</sup> To date, phospholipid monolayer insertion studies have only been performed for the proapoptotic Bid molecule.<sup>23</sup>

In the present study, we investigated the membrane insertion property of the antiapoptotic protein Nr-13 independent of its putative membrane targeting hydrophobic sequence. Nr-13 is a Bcl-2-related protein involved in neoplastic transformation by the *v-src* oncogene.<sup>24</sup> It plays a major role in the regulation of cell death in B-cells during the development of the immune system in the chicken bursa.<sup>25</sup> Previous studies have established that the recombinant Nr-13 protein lacking the C terminal hydrophobic domain maintains its antiapoptotic function, and have shown that Nr-13 interacts with high affinity with the BH3 domain of Bax, and completely counteracts the death-inducing activity of this domain.<sup>26</sup> Besides, it has been proposed that Nr-13, *via* its direct interaction with cytochrome *c*, may ensure the maintenance of mitochondrial integrity, and prevent apoptosis.<sup>26</sup> In previous studies, full-length Nr-13 was shown to be localized at the mitochondrial level,<sup>27</sup> and to interact specifically with Bax in vertebrate cells.<sup>25,27</sup> Molecular modeling of Nr-13 suggests a structural pattern similar to Bcl-x<sub>L</sub>.<sup>27</sup> Here, we determine the cross-sectional area of the Nr-13 molecule inserted into the phospholipid monolayer, and show that the lipid penetration of Nr-13 occurs *via* the total cross-section of the molecule. Thus, for the first time, we elucidated the size of an antiapoptotic protein embedded into a membrane model. Furthermore, we demonstrated that the heterodimer formed by Nr-13 and BH3 domain of proapoptotic Bax, could no longer penetrate into the phospholipid monolayer. This insight into the localization of the heterodimer complex suggests that antiapoptotic Nr-13 and proapoptotic proteins exerts their antagonistic effects by preventing each other from reaching the membrane.

## Results and Discussion

### Interaction of Nr-13 with monomolecular film

The aim of this study was to determine the capacity of Nr-13, lacking its putative membrane targeting domain, to penetrate into the monolayers.

For this purpose, the C terminal stretch of 20 hydrophobic residues was removed from the Nr-13 ( $\Delta$ TM). The interaction of Nr-13  $\Delta$ TM (termed Nr-13 hereafter) with lipid monolayers was analyzed using Langmuir film balance technology. In these experiments, Nr-13 was added at constant area set-up, to the aqueous subphase underneath a monomolecular lipid film, and the resulting interaction was measured as an increase in the surface pressure of the film. This increase reflects insertion of part of the protein between the phospholipid molecules, and not its peripheral attachment to the lipid head groups. The lipid specificity of the protein insertion was first investigated by injection of Nr-13 under different types

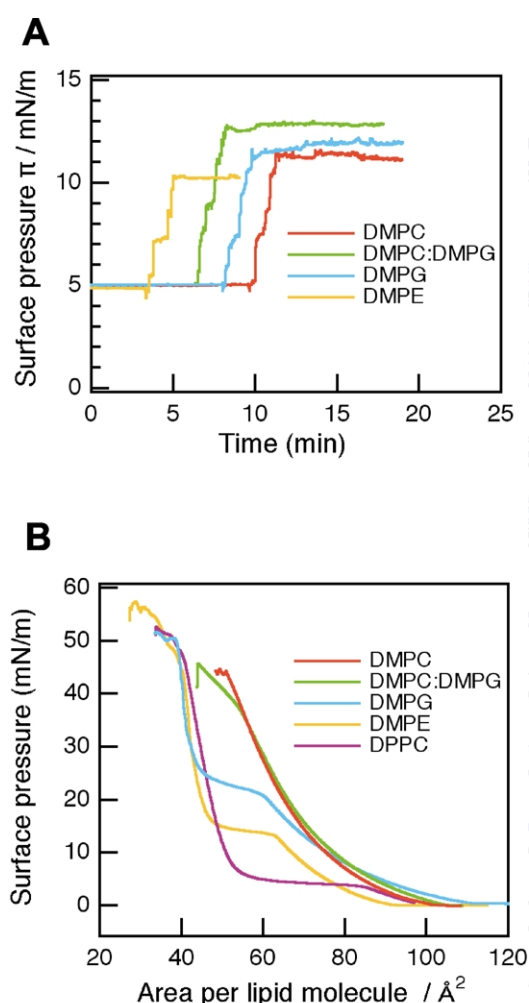


**Figure 1.** Interaction between Nr-13  $\Delta$ TM and different monomolecular films. A, Time-course of the monolayer insertion of wild-type NR-13, upon injection of 10 nM Nr-13 underneath the monolayer, at an initial surface pressure of 5 mN/m. Changes in surface pressure were recorded at constant area and temperature (26 °C). Different monolayers used were: DMPC (26.1 nmol), DMPE (24.5 nmol), DMPG (24.5 nmol), and mixed DMPC/DMPG in an 8/2 molar ratio (a total of 22.9 nmol). B, Compression isotherm of the above monolayers on pure water subphase at 26 °C. In addition, the compression isotherm of DPPC is shown.

of lipid monolayers. Nr-13 insertion gave rise to an immediate surface pressure increase (Figure 1A), while no surface pressure change was observed upon injection of either the buffer in which Nr-13 was stored, or the Nr-13 in the subphase in the absence of lipid (data not shown). Nr-13 insertion resulted in a slightly higher surface pressure changes in DMPC and DMPG monolayers than in DMPE monolayer (Figure 1A). Interestingly, the greatest pressure increase was observed in mixed DMPC/DMPG (8/2) monolayers, illustrating the specificity of the interaction with the outer mitochondrial membrane which contains mostly zwitterionic phospholipids (PC head group) and a small percentage of negatively charged lipids.<sup>28</sup> The phase behavior of these monomolecular films was presented by their compression isotherms on pure water (Figure 1B). At low pressure, they were present in the liquid-expanded (LE) phase, associated with membrane fluidity, a requisite in the investigation of the protein interaction with lipid membranes. However, it is worthwhile noting that, upon compression, both DMPG and DMPE monolayers underwent a transition to the liquid-condensed (LC) phase, marked by a plateau region in their isotherms corresponding to LE/LC coexistence. Whereas, DMPC monolayer remained in the LE phase, the naturally occurring DPPC condensed into the LC phase at very low surface pressure at 26 °C (Figure 1B). In the mixed DMPC/DMPG monolayers, the influence of a condensed DMPG domain in the fluid DMPC monolayer cannot be excluded, since a kink in the isotherm was observable at  $\pi$  around 40 mN/m (Figure 1B). Thus, although negatively charged lipids have been reported to be necessary for the efficient interaction of recombinant Bcl-2 family proteins with model membranes,<sup>12,18,20,21</sup> the penetrating behavior of Nr-13 was further studied using a DMPC monolayer because of its fluidity, and because PC is the major head group among outer mitochondrial membrane phospholipids.<sup>28</sup>

Nr-13 was found to interact with DMPC in a dose-dependent manner (Figure 2A). The maximal surface pressure increase ( $\Delta\pi$  max = 10 mN/m) was reached with a Nr-13 concentration as low as 15 nM, and a half-maximal increase was reached at 2.3 nM. For convenience, these experiments were carried out at 22 °C. Experiments performed at various temperatures, showed that the increase of temperature up to 30 °C, did not influence the penetrating behavior of Nr-13 (data not shown). At the more physiologically relevant temperature of 35 °C, precise surface measurements could not be performed due to rapid subphase evaporation. To assess the stability of the lipid-protein interaction, pressure-area isotherms of Nr-13-containing monolayers were studied (Figure 2B). At surface pressures below 25 mN/m, the isotherm obtained in the presence of Nr-13 shifted to larger areas per molecule (broken line) compared to the pure lipid isotherm (continuous line). This increase arose from the area occupied by the protein.

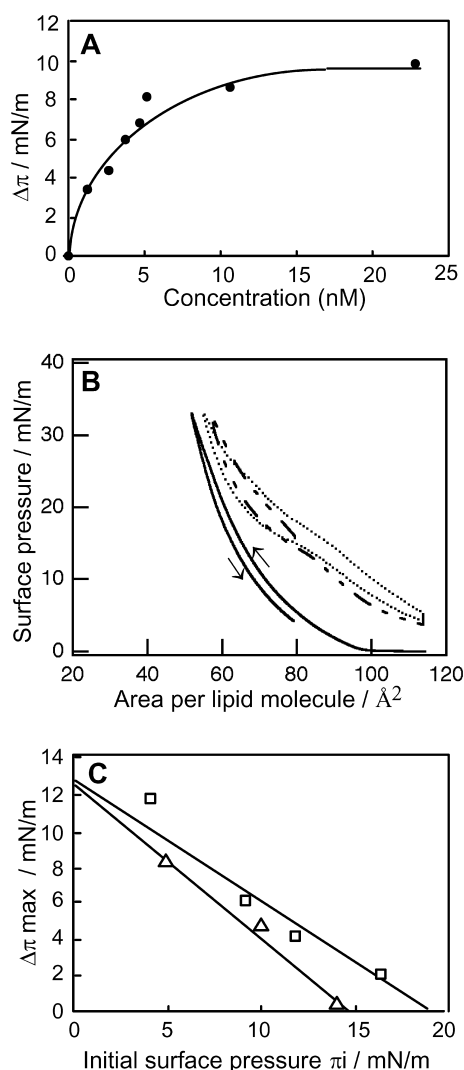


**Figure 2.** Interaction between Nr-13  $\Delta$ TM and a monomolecular film of DMPC. A, Increase in surface pressure, upon injection of the indicated concentrations of Nr-13 underneath the monolayer, at an initial pressure of 5 mN/m. B, Compression/expansion isotherm cycles of a DMPC monolayer (23.4 nmol) on pure buffer subphase (continuous line, follow the arrows), after injection of Nr-13 (15 nM) at an initial pressure of 5 mN/m and waiting for the equilibrium surface pressure to reach 15 mN/m (broken line), and followed by a second cycle beginning at a surface pressure of 6 mN/m after complete expansion of the mixed monolayer (dotted line). C, Maximal surface pressure increase ( $\Delta\pi_{\text{max}}$ ), reached after injection of 15 nM of either wild-type Nr-13 (open squares) or Nr-13QAQ (open triangles) underneath the DMPC monolayer, as a function of various initial surface pressures ( $\pi_i$ ). Experiments were performed at 22 °C. Each point is an independent measurement with a new lipid monolayer. Representative data from two or three independent experiences are shown.

Although, the shift was less pronounced above 25 mN/m, suggesting that part of Nr-13 was squeezed out, it should be noted that Nr-13 was still present in the monolayer even at high pressure. On lowering the surface pressure, the lipid monolayer was expanded by reincorporating

Nr-13 reversibly into the monolayer (broken line). A second compression/expansion cycle led to a very similar isotherm, confirming the stability of the lipid–protein interaction (dotted line), as reported for other proteins.<sup>29</sup>

To examine the lipid penetration process further, monolayers of DMPC were prepared at various initial pressures ( $\pi_i$ ), then the surface pressure increase ( $\Delta\pi$ ) induced by Nr-13 (15 nM) was determined following attainment of equilibrium. Higher initial monolayer surface pressures correlated with higher lipid packing densities and consequently reduced penetrative power of the protein. As expected, Figure 2C (squares) shows that  $\Delta\pi$  gradually decreased as  $\pi_i$  increased. The critical pressure of insertion (i.e. the theoretical value of  $\pi_i$  extrapolated for  $\Delta\pi = 0$  mN/m) was 19 mN/m. Such an influence of the initial packing density of the lipid monolayer on Nr-13 penetration demonstrates a direct Nr-13/lipid interaction, as established for several other lipids and ligands,<sup>30</sup> even though the critical pressure did not reach the lateral pressure reported for biological membranes<sup>31</sup> (30 mN/m). Nonetheless, it is worthwhile to remember that when inserted, the Nr-13 protein remained in the phospholipid even at high surface pressure (see Figure 2B). It should be noted that many of the previously reported studies on membrane insertion of Bcl-2  $\Delta$ TM proteins were performed indirectly by measuring the multiconductance function of channels formed by these proteins in lipid vesicles or planar membranes.<sup>5,10</sup> Our data show evidence for a direct insertion of an antiapoptotic Bcl-2 protein, devoid of its C-terminal membrane binding domain, into a lipid monolayer, which may be considered a basic biomembrane model. In addition, the Nr-13/lipid interaction occurred at physiological pH, in contrast to the binding of Bcl-2 ( $\Delta$ TM) and Bcl-x<sub>L</sub>( $\Delta$ TM) to lipid vesicles which only occur at acidic pH.<sup>12,18–20</sup>

### Phospholipid penetration area correlates with the entire Nr-13 molecular cross-section

Since the central  $\alpha 5$ – $\alpha 6$  helices seem to play an essential role in membrane insertion,<sup>10,15</sup> their possible contribution was evaluated by measuring the molecular cross-section of Nr-13 section inserted into the lipid monolayer. Such information may permit the identification of the limits of the domains inserted into the membrane. In these experiments, a known amount of DMPC ( $n_L$ ) was spread onto the buffer surface, and the phospholipid monolayer, with a given initial area was maintained under a constant low surface pressure during penetration measurement. Following injection of the protein into the buffer subphase, insertion of the protein into the lipid monolayer gave rise to an increased lipid area  $\Delta A$ . Figure 3A (continuous line) shows the increase of DMPC area as a function of time following insertion of Nr-13, with the surface pressure remained constant at 5 mN/m (broken line). At this low pressure, a



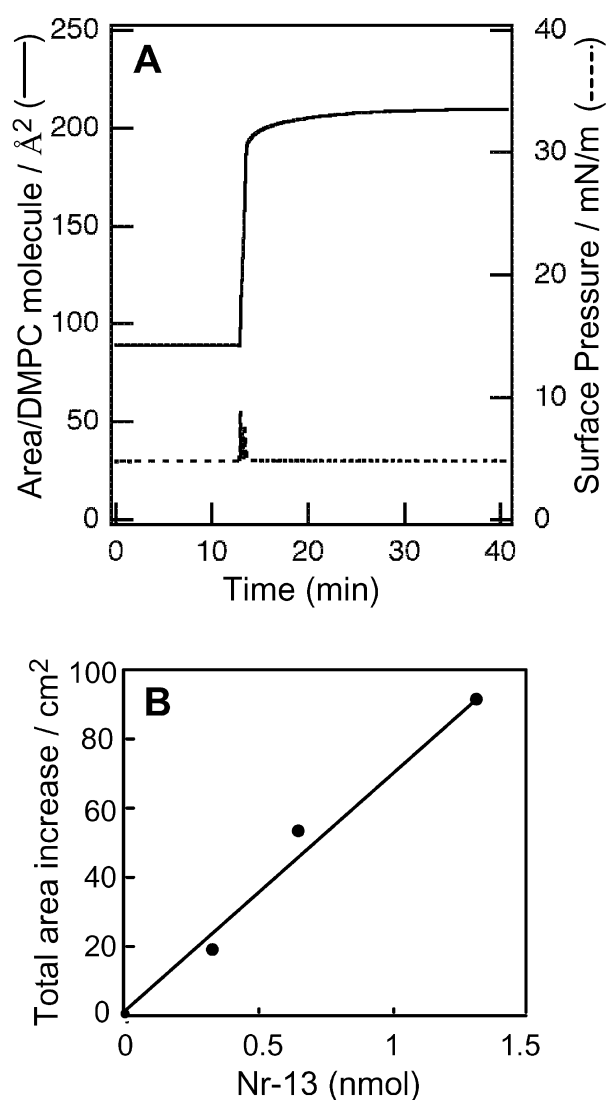


**Figure 3.** Penetration of Nr-13  $\Delta$ TM into a DMPC monolayer. A, Lipid area increase in  $\text{\AA}^2$ /DMPC molecule *versus* time after injection of 1.3 nmol of Nr-13 beneath the DMPC monolayer (12.6 nmol, continuous line), at 22  $^{\circ}\text{C}$ . The surface pressure was maintained constant at 5 mN/m through the experiment (broken line). The equilibration time was 10–20 minutes. After reaching equilibrium, the area expansion per lipid molecule ( $\Delta A$ ) was calculated to be equal to  $120.8 \text{ \AA}^2$ . Considering the total number of DMPC molecules forming the monolayer ( $n_L = 75.88 \times 10^{14}$ ), the total area increase ( $\Delta A \times n_L$ ) will be  $91.6 \times 10^{16} \text{ \AA}^2$ . B, Relationship between total surface area increase in  $\text{cm}^2$  ( $\Delta A \times n_L$ , calculated as above) and the indicated amounts of Nr-13 (nmol) injected as in A. The cross-section area of Nr-13 ( $A_p$ ) can be calculated from the slope of the total area increase *versus* the total number of Nr-13 molecules ( $n_p$ ). Representative data obtained from two independent experiments are presented.

linear increase in total area ( $\Delta A \times n_L$ ) can be observed, as illustrated in Figure 3B, after injection of increasing amounts of Nr-13. The observed linearity reflects practically complete interfacial protein/lipid “binding”, resulting in no loss of protein into the subphase.<sup>32</sup> Therefore, the molecular cross-section

occupied by the protein can be simply derived from the slope of the total area increase *versus* number of protein molecules  $n_p$ . Consequently, at 5 mN/m, the molecular cross-section of Nr-13 inserted in the DMPC monolayer corresponds to  $1100 \text{ \AA}^2$ . This is the first estimation of the size of a Bcl-2 protein inserted into a phospholipid monolayer. Such a cross-section indicates that the boundary of Nr-13 involved in monolayer insertion is much greater than that of the plane perpendicular to the two  $\alpha 5$ – $\alpha 6$  helices ( $320$ – $340 \text{ \AA}^2$ ), since the area per helix, deduced from surface pressure experiments at the air/water interface,<sup>33</sup> does not exceed  $160$ – $170 \text{ \AA}^2$ . In parallel, assuming Nr-13 to be a globular protein with a molecular mass of 17768 Da occupying  $0.73 \text{ cm}^3/\text{g}$ , its calculated cross-section would be  $936 \text{ \AA}^2/\text{molecule}$ , which is close to the above experimental values. Our results strongly suggest that the entire cross-section of Nr-13, involving domains in addition to the two hairpin helices alone, is involved in insertion of this antiapoptotic protein into the monolayer. This is consistent with NMR studies on Bcl-x<sub>L</sub> in micelles, showing that a helix other than 5 or 6 is also buried within the membrane.<sup>34</sup>

The potential for Nr-13 domains to be buried in the hydrophobic interior of the monolayer was examined using helical wheel projection (Figure 4), based on the structure of human Bcl-x<sub>L</sub><sup>15</sup> and the predicted structure of quail Nr-13.<sup>27</sup> While helix 1 cannot be considered as amphipathic (Figure 4A), helix 2 shows some amphipathic character (Figure 4B). Helix 4 is strongly amphipathic with its charged residues concentrated on one side of the helix (Figure 4C). The equivalent of Bcl-x<sub>L</sub> helix 3 is missing from the predicted structure of Nr-13. As in the central helices of other Bcl-2 proteins, and in accordance with molecular modeling of Nr-13 showing that the central helices present potential membrane insertion domain,<sup>27</sup> the  $\alpha 5$ – $\alpha 6$  helices are strongly amphipathic (not shown). From a structural point of view, the overall amphipathicity of these domains, added to the previously described hydrophobic behavior of the protein,<sup>26</sup> reinforce the tendency of Nr-13 to penetrate into lipid monolayers/membranes. Furthermore, the amino acid sequence motif GxxxG has been reported to stabilize helix–helix interaction in membrane proteins,<sup>35</sup> Nr-13 possesses three such motifs in its sequence (80–84, 104–108, 132–136) instead of one in Bcl-x<sub>L</sub> sequence. These motifs may help stabilizing the protein fold when inserted into the membrane.

### Phospholipid interaction of a Nr-13 mutant

To further explore the membrane insertion of the  $\alpha 5$ – $\alpha 6$  helices, a mutation was designed in which three acidic Glu residues (E102, E106, and E107), in the  $\alpha 5$ – $\alpha 6$  connecting loop (Figure 5A and B) were changed to Gln, Ala, and Gln (QAQ mutation). A structure prediction search revealed no change in hairpin structure of the helices in such a mutant, except for a connecting loop somewhat longer than

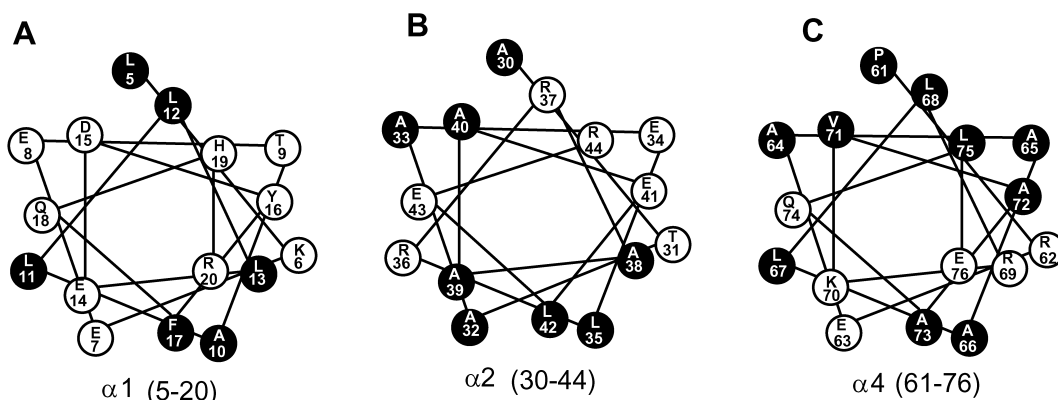


**Figure 4.** Helical wheel projection of  $\alpha$ -helices 1(A), 2(B) and 4(C) of chick Nr-13. The predicted structure of quail Nr-13,<sup>26</sup> presenting 96% sequence identity with chick Nr-13, and the coordinates of Bcl-x<sub>L</sub> (from the Protein Data Bank) were used to determine helical domains. Hydrophobic residues are in black, hydrophilic residues in white.

in wild-type (Figure 5, compare A and B). In addition, circular dichroism spectroscopy shows that the purified mutant protein displayed  $\alpha$ -helical structure, similar to that of wild-type Nr-13,<sup>26</sup> with the characteristic negative bands at 208 and 222 nm (Figure 5C). The aim of this mutation was to neutralize the charge on the acidic residues, since, in the structurally related diphtheria toxin pore-forming domain, mutations of similar acidic residues at the tip of the helical hairpin have been shown to be sufficient to alter helix membrane insertion.<sup>36</sup> The interaction of Nr-13QAQ with a DMPC monolayer was analyzed by measuring the increase in surface pressure induced by protein insertion. Unexpectedly, this charge-neutralized mutant protein was

found to interact with DMPC, reaching a maximal surface pressure increase of 9 mN/m with 10 nM Nr-13QAQ, and a half-maximal increase with 1.6 nM (Figure 5D), thus exhibiting values comparable to wild-type Nr-13 (compare Figures 2A and 5D). The measurement of surface pressure increase as a function of initial pressure of the DMPC monolayer, shown in Figure 2C (open triangles), indicated a critical insertion pressure of 15 mN/m for Nr-13QAQ. For an initial pressure of 11 mN/m, the increase in surface pressure was 5.6 mN/m for wild-type but only 3 mN/m for the QAQ mutant (Figure 2C, compare open squares and triangles), indicating that the mutant interacted with the monolayer, yet less efficiently than wild-type

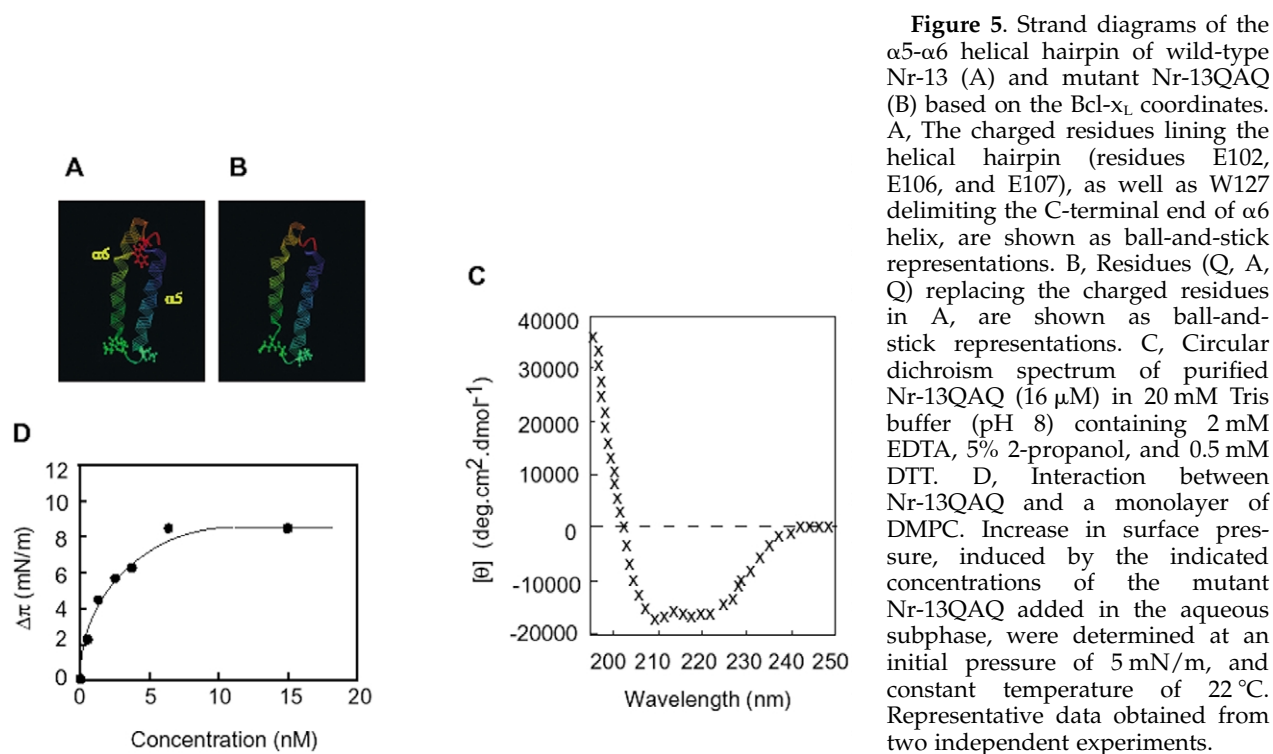


**Figure 5.** Strand diagrams of the  $\alpha$ 5- $\alpha$ 6 helical hairpin of wild-type Nr-13 (A) and mutant Nr-13QAQ (B) based on the Bcl-x<sub>L</sub> coordinates. A, The charged residues lining the helical hairpin (residues E102, E106, and E107), as well as W127 delimiting the C-terminal end of  $\alpha$ 6 helix, are shown as ball-and-stick representations. B, Residues (Q, A, Q) replacing the charged residues in A, are shown as ball-and-stick representations. C, Circular dichroism spectrum of purified Nr-13QAQ (16  $\mu$ M) in 20 mM Tris buffer (pH 8) containing 2 mM EDTA, 5% 2-propanol, and 0.5 mM DTT. D, Interaction between Nr-13QAQ and a monolayer of DMPC. Increase in surface pressure, induced by the indicated concentrations of the mutant Nr-13QAQ added in the aqueous subphase, were determined at an initial pressure of 5 mN/m, and constant temperature of 22  $^{\circ}$ C. Representative data obtained from two independent experiments.

Nr-13. However, Nr-13QAQ was as active as wild-type Nr-13<sup>26</sup> in the prevention of caspase-3 activation in cell-free extract assays (data not shown). Several studies focused on the region surrounding the  $\alpha 5$ - $\alpha 6$  helices of other Bcl-2 family members<sup>37,38</sup> have reported a similar attenuated effect upon mutation. Our data, in accordance with these studies suggest that the region surrounding these  $\alpha 5$ - $\alpha 6$  helices is essential for optimal interaction with the monolayer. However, the charge neutralization within this region did not abolish Nr-13 insertion into the phospholipid monolayer. This result is not consistent with the pore-forming model proposed for Bcl-2 proteins, since, based on structural homology with diphtheria toxin,<sup>15</sup> charge neutralization should probably alter membrane insertion.<sup>36</sup> Therefore, this result and the finding that the lipid insertion area of Nr-13 corresponds to the entire cross-section of the molecule, may in fact favor other models by which Nr-13 helps promote mitochondrial homeostasis.

### The proapoptotic BH3 domain inhibits the phospholipid insertion of Nr-13

The high-affinity phospholipid insertion of antiapoptotic Nr-13 raised the question of how heterodimerization with proapoptotic domain could take place within the hydrophobic environment of the membrane. One of the essential functions of antiapoptotic Bcl-2 proteins is to counteract the activity of proapoptotic members through heterodimerization *via* the latter's BH3 domain.<sup>1,3,4</sup> However, the mechanism whereby these heterodimers integrate into the biological membranes remains obscure. Thus, to elucidate the membrane insertion behavior of the antiapoptotic protein Nr-13 complexed with the BH3 domain of the proapoptotic protein Bax, the lipid monolayer insertion of wild-type Nr-13, in the presence or absence of the BH3 peptide, was studied by measuring the surface pressure increase of a DMPC monolayer kept at constant surface area. In a preliminary experiment, it was verified that injection of the BH3 peptide alone, at a low concentration (15 nM), into the subphase did not produce any increase in surface pressure of the monolayer (data not shown). **Figure 6A** (continuous line) shows the surface pressure increase of the DMPC monolayer resulting from insertion of Nr-13, as a function of time. When Nr-13 was pre-incubated for ten minutes with a stoichiometric molar ratio of BH3 peptide, a net smaller increase in surface pressure was observed (**Figure 6A**, broken line), suggesting that dimerization drastically diminished monolayer insertion. Nr-13/ BH3 dimerization has been reported to occur with high affinity ( $K_D = 3 \times 10^{-7}$  M).<sup>26</sup> To confirm the specificity of the interaction, similar injections were performed in the presence of an unrelated peptide, leading to a similar surface pressure increase to that with Nr-13 alone (**Figure 6A**, dotted line). The unrelated peptide presents, like BH3 peptide, a strong

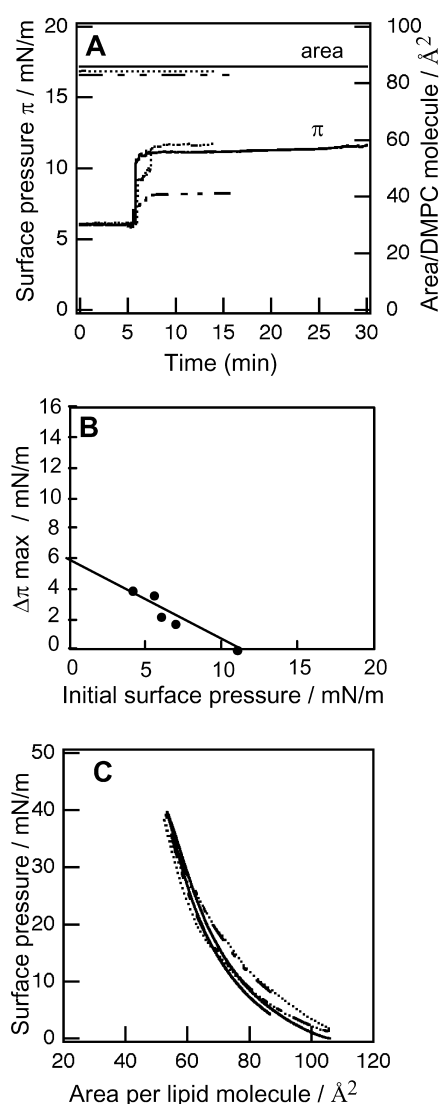


**Figure 6.** Effect of the specific interaction of the proapoptotic BH3 domain on monolayer penetration of Nr-13. **A**, Time-course of the DMPC monolayer insertion of wild-type Nr-13 before (continuous line), after a ten-minute incubation with a stoichiometric molar ratio of Bax BH3 peptide (broken line), and after incubation with an unrelated peptide at the same stoichiometric molar condition (dotted line). Changes in surface pressure were recorded at constant area. **B**, Maximal surface pressure increase ( $\Delta\pi_{\text{max}}$ ) induced by injection of the Nr-13/BH3 complex underneath the DMPC monolayer, as a function of various initial surface pressures ( $\pi_i$ ). **C**, Compression/expansion isotherm cycles of a DMPC monolayer (25.2 nmol) on a pure buffer subphase (continuous line), after injection of Nr-13/BH3 complex (formed by incubation of stoichiometric molar ratio of Nr-13 and BH3 peptide, broken line), and followed by a second cycle after complete expansion of the monolayer (dotted line). Each experiment was performed at 22 °C, with a constant Nr-13 concentration of 14.6 nM.

potential to form  $\alpha$ -helical structure (70–80%) as determined by secondary structure prediction and shows some amphipathic character (data not shown), therefore, validating the use of this peptide as control.



When phospholipid insertion was analyzed at various initial surface pressures ( $\pi$ ), the maximal surface pressure increase with the Nr-13/BH3 complex remained low, with a critical insertion pressure of 11 mN/m, indicating that the complex had little (if any) effect of DMPC monolayer pressure (Figure 6B). Therefore, the Nr-13/BH3 complex appears to be essentially unable to penetrate the lipid interface. This was confirmed by studying pressure–area isotherms of the complex-containing monolayer (Figure 6C). Only a slight shift to larger areas was observed in the presence of Nr-13/BH3 complex, at surface pressures below 20 mN/m (Figure 6C). Above this pressure, a substantial squeeze out of the complex from the monolayer was observed. These data indicate that when Nr-13 undergoes heterodimerization with the proapoptotic BH3 domain, it loses its capacity to be inserted into phospholipid monolayers/membranes. On the contrary, after insertion of Nr-13 into the DMPC monolayer, injection of a high concentration of BH3 peptide (1  $\mu$ M) under the subphase did not produce further changes in surface pressure (data not shown), even though, at such high concentrations the BH3 peptide can reach and penetrate into the membrane.<sup>39</sup> Therefore, the heterodimerization cannot occur within the membrane, and the BH3 peptide cannot reach and interact with Nr-13 once Nr-13 is inserted into the monolayer. Recently, other studies, based on measurements of membrane curvature, have shown the membrane insertion behavior of proapoptotic tBid and the inhibiting effect of antiapoptotic Bcl-x<sub>L</sub>.<sup>40</sup> Nonetheless, the positioning of the antiapoptotic/proapoptotic complex with regard to the membrane has never been elucidated. Our data indicate that while wild-type as well as mutated Nr-13 are able to interact efficiently with a DMPC monolayer, Nr-13 heterodimerization with the proapoptotic BH3 domain occurs out of the monolayer/membrane, and specifically inhibits its partitioning into the membrane.

The main finding of this study is that we established a direct, specific and stable interaction between the antiapoptotic protein Nr-13, devoid of its putative transmembrane domain, and the phospholipid monolayer DMPC at the air–water interface, using Langmuir balance technology. We demonstrated that protein penetration into the lipid occurs in such a way that the entire cross-section of Nr-13 covering 1100 Å<sup>2</sup>/molecule is embedded into the monolayer. Furthermore, we showed that the monolayer insertion of Nr-13 is not dependent on the negatively charged residues within the loop connecting the central helices, as established for bacterial pore-forming proteins.<sup>36</sup> These findings call into question the pore-forming role attributed to the central  $\alpha$ 5– $\alpha$ 6 helices of antiapoptotic proteins, and their concomitant channel activity. Our data favor a model in which the antiapoptotic molecule inserted into the membrane may help ensure mitochondrial integrity. The promotion of mitochondrial homeostasis, considered

as one of the functions of antiapoptotic Bcl-2 proteins,<sup>1,4</sup> would further support such a model.

Another outcome of this study is the finding that heterodimerization of antiapoptotic Nr-13 with the BH3 domain of proapoptotic Bax inhibits phospholipid insertion, and that heterodimerization cannot occur within the membrane. It is worth remembering that proapoptotic proteins exert their functions at the level of outer mitochondrial membrane.<sup>5–7</sup> Studies with different experimental systems have given rise to a wide variety of mechanisms to explain membrane permeabilization by proapoptotic Bcl-2 members, including ion channel activity,<sup>10–12</sup> destabilization of lipid bilayer,<sup>21</sup> and interaction with components of the permeability transition pore (PTP<sup>41</sup>). Nonetheless, few studies have focused on their membrane insertion capacity upon heterodimerization with Bcl-2 antiapoptotic members. To understand how a membrane-bound antiapoptotic protein could prevent apoptosis by

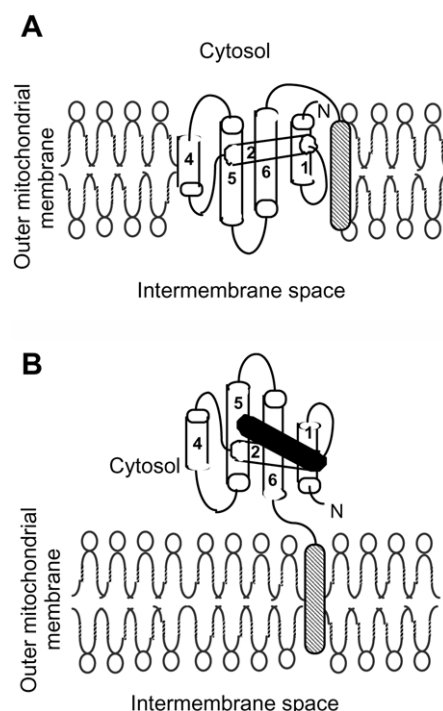


**Figure 7.** Schematic representation of Nr-13 localization with respect to the membranes, in the absence (A), and presence (B) of BH3 domain of Bax. A, In the absence of apoptotic stimuli, the helical structure of Nr-13 embedded into outer membrane through its entire cross-section involving other helical domains, in addition to the hairpin helices ( $\alpha$ 5 and  $\alpha$ 6). The structure of Nr-13 was based on its previously reported molecular modeling.<sup>27</sup> N indicates the N terminus of the molecule. The C-terminal hydrophobic transmembrane domain is indicated by hatched gray box. B, In the presence of apoptotic stimuli, Nr-13 leaving the mitochondrial membranes after heterodimerization with BH3 domain of Bax (black box). The heterodimer localization becomes cytosolic. However, the full-length Nr-13 remains anchored to the membrane by its C-terminal transmembrane domain, maintaining the Nr-13/Bax heterodimer close to the membrane.

binding, at the cytosolic level, a BH3 domain proapoptotic protein, a hypothetical model can be proposed (Figure 7). According to this model, in the absence of apoptotic stimuli, Nr-13 is inserted into the membrane, in addition to its C-terminal transmembrane domain, *via* amphipathic helical domains, as mentioned above (Figure 7A). After an apoptotic signal, the antiapoptotic Nr-13, presenting high affinity for proapoptotic BH3 domain,<sup>26</sup> interacts strongly with this domain to form a heterodimer, and counteracts the proapoptotic proteins, including BH3-only proteins, by preventing them from reaching the outer mitochondrial membrane (Figure 7B). According to this model, the squeeze out of Nr-13 from the membrane seems to be a prerequisite for the heterodimerization; however, at this stage, the processes that drive this extraction remain unknown. In this model, it is assumed that the C-terminal tail of Nr-13 remains anchored to the membrane, and maintains the cytosolic Nr13/BH3 complex close to the membrane/cytosol interface (Figure 7B). This model is consistent with recent studies on the supramolecular openings of the outer mitochondrial membrane by BH3/Bax/lipid interaction, which is inhibited by Bcl-x<sub>L</sub>.<sup>42</sup> At this stage, we can only speculate on the mechanism of the Nr-13 mode of action. It is still not known whether it is the antiapoptotic Nr-13 protein that counteracts apoptotic activity by preventing proapoptotic proteins from reaching the membrane, or the proapoptotic proteins that inhibit the maintenance of mitochondrial homeostasis, ensured by antiapoptotic Nr-13, by maintaining it out of the membrane. However, a new insight into the localization of the heterodimer complex has been introduced.

## Materials and Methods

### Plasmid constructions and protein purification

Wild-type Nr-13  $\Delta$ TM was produced as described,<sup>26</sup> lacking the 20 most C-terminal residues, bearing additional Leu Gln residues, and His tag (six His) at its C terminus. The protein was stored in a buffer containing 20 mM Tris (pH 8.0), 0.15 M NaCl, 2 mM EDTA, 10 mM DTT and 5% (v/v) 2-propanol. For the Nr-13QAQ mutant, a two-steps PCR procedure was used. First, two mutated overlapping PCR products (nucleotides 1–339 and 286–471) were obtained by separate reactions using wild-type Nr-13 as template. Fragment 1–339 was generated using forward wild-type primer including an *NdeI* site at the 5' end, and a reverse primer with substituted codons as follows: Glu102 (GAG) with Gln (CAA), Glu106 (GAG) with Ala (GCA), and Glu107 (GAA) with Gln (CAA). Fragment 286–471 was generated using a mutagenic forward primer introducing the above-mentioned substituted codons, and a wild-type reverse primer including a *PstI* site at the 3' end. Both fragments were mixed, then allowed to hybridize (5 minutes at 50 °C) and elongate (ten minutes at 72 °C) for the generation of the mutated template. Finally, this template was used in a last PCR step to generate Nr-13QAQ, using the above forward and reverse wild-type primers.

The final PCR product was cloned into the *NdeI* and *PstI* sites of the pT7-7 plasmid encoding six His codons followed by a stop codon downstream of the *PstI* site. The coding regions of the plasmid were sequenced to confirm the absence of extra mutations. As for wild-type Nr-13, the mutant protein lacked the C-terminal hydrophobic transmembrane region. Overexpression and purification of the mutant protein were performed as previously described for wild-type Nr-13.<sup>26</sup>

### Peptide synthesis

The synthesis of the BH3 peptide (VPQDASTKK LSECLKRIGDELDSNMELQR) corresponding to the BH3 domain (underlined) of human proapoptotic Bax was reported elsewhere.<sup>26</sup> The non-relevant peptide (PWVAPMRMRVRLMLETMFL) was synthesized as reported for the BH3 peptide.

### Surface pressure measurements

A Wilhelmy balance was used to measure protein-induced changes in the surface pressure of a monomolecular film of phospholipids at constant surface area. The surface pressure was measured using a Langmuir round Teflon trough (Riegler & Kirstein, Germany). The surface pressure,  $\pi = \gamma_0 - \gamma$ , where  $\gamma_0$  is the surface tension of pure buffer and  $\gamma$  the surface tension of protein solution, was monitored using Whatman no. 1 filter-paper, connected to the Wilhelmy balance. Experiments were carried out in a controlled atmosphere at either 22 °C or 26 °C. The apparatus allowed the recording of pressure–area compression/expansion isotherm cycles and the kinetics of interaction of a ligand with the monomolecular film.

A monomolecular film was formed by spreading the lipid (DMPC, DMPG, DMPE, DPPC, Sigma) dissolved in chloroform/methanol (9:1, v/v) on the buffer subphase, then allowing the solvent to evaporate for about 15 minutes. In all experiments, the subphase was 120 ml of 20 mM Tris–HCl, (pH 7.5), 0.15 M NaCl and 1 mM DTT, continuously stirred with a magnetic stirring bar. To measure the interaction of Nr-13 with lipid monolayers, various concentrations of protein were injected using a Hamilton syringe into the buffer subphase, between fixed barriers (imposing a constant area), and surface pressure increases produced were recorded. Each injection was performed with a fresh film and subphase.

The area available to a monolayer can be decreased by imposing an external compression through mobile barriers. For recording the isotherms, the surface pressure was measured as a function of surface area. A typical experiment was carried out as follows: after spreading the phospholipid molecules, compression was started after a long waiting period to allow solvent evaporation. Having reached the maximum compression (usually at 40 mN/m), the DMPC monolayer was then expanded back to the original area corresponding to the initial surface pressure chosen for subsequent protein insertion. After an appropriate waiting period to allow monolayer relaxation, the protein was injected and, when a new surface pressure equilibrium was reached, the next isotherm was recorded. A series of isotherms were thus recorded, starting with a given amount of pure lipid, followed by two isotherms with added protein.

### Measurement of protein penetration cross-sectional area

After spreading of a known number of DMPC molecules,  $n_L$ , as above, various concentrations of Nr-13 were injected into the buffer subphase between two movable barriers, where the surface pressure,  $\pi$ , was maintained constant by means of an electronic feedback system. Penetration of protein molecules into the monolayer gives rise to an area expansion  $\Delta A$ . Assuming, at low pressures, that all protein molecules,  $n_p$ , remain integrated in the monolayer, the cross-sectional area  $A_p$  of the protein portion inserted into the lipid monolayer, corresponds to:

$$\Delta A \times n_L = A_p \times n_p \quad (1)$$

According to equation (1), the molecular cross-section may be determined from the slope of the total expanded area ( $\Delta A \times n_L$ ) versus  $n_p$ .

### Structure analysis

The predicted structures of  $\alpha 5$ - $\alpha 6$  helical hairpin (residues G80-F138) of Nr-13 was modeled, based on the coordinates available for Bcl-x<sub>L</sub> (Protein Data Bank entry 1MAZ), using Geno3D<sup>†</sup>. For CD measurements, 17  $\mu$ M Nr-13QAQ samples in 20 mM Tris (pH 8.0), 2 mM EDTA, 5% 2-propanol, and 0.5 mM DTT were used. CD spectra were recorded as described.<sup>26</sup>

### Acknowledgements

The authors thank Dr F. Letourneur for helpful discussions for the cloning strategy, and D. Hulmes for critical reading of the manuscript. This work was supported by La Ligue Nationale Contre le Cancer and comité de la Drôme, the Association pour la Recherche sur le Cancer, the Centre National de la Recherche Scientifique and the Université Claude Bernard Lyon 1.

### References

- Cory, S. & Adams, J. (2002). The Bcl-2 family: regulators of the cellular life-or-death switch. *Nature Rev.* **2**, 647–656.
- Kluck, R. M., Bossy-Wetzel, E., Green, D. R. & Newmeyer, D. D. (1997). The release of cytochrome c from mitochondria: a primary site for Bcl-2 regulation of apoptosis. *Science*, **275**, 1132–1136.
- Wang, X. (2001). The expanding role of mitochondria in apoptosis. *Genes Dev.* **15**, 2922–2933.
- Gross, A., McDonnell, J. M. & Korsmeyer, S. J. (1999). Bcl-2 family members and the mitochondria in apoptosis. *Genes Dev.* **13**, 1899–1911.
- Martinou, J. C. & Green, D. R. (2001). Breaking the mitochondrial barrier. *Nature Rev. Mol. Cell Biol.* **2**, 63–67.
- Esques, R., Desagher, S., Antonson, B. & Martinou, J. C. (2000). Bid induces the oligomerization and insertion of Bax into the outer mitochondrial membrane. *Mol. Cell Biol.* **20**, 929–935.
- Nechushtan, A., Smith, C. L., Lamensdorf, I., Yoon, S. H. & Youle, R. J. (2001). Bax and Bak coalesce into novel mitochondria-associated clusters during apoptosis. *J. Cell Biol.* **153**, 1265–1276.
- Grinberg, M., Sarig, R., Zaltsman, Y., Frumkin, D., Grammatikakis, N., Reuveny, E. & Gross, A. (2002). tBid homooligomerizes in the mitochondrial membrane to induce apoptosis. *J. Biol. Chem.* **277**, 12237–12245.
- Cheng, E. H., Wei, M. C., Weiler, S., Flavell, R. A., Mak, T. W., Lindsten, T. & Korsmeyer, S. J. (2001). Bcl-2, Bcl-x(L) sequester BH3 domain-only molecules preventing Bax- and Bak-mediated mitochondrial apoptosis. *Mol. Cell.* **8**, 705–711.
- Schendel, S., Montal, M. & Reed, J. C. (1998). Bcl-2 family proteins as ion-channels. *Cell Death Differ.* **5**, 372–380.
- Saito, M., Korsmeyer, S. J. & Schlesinger, P. H. (2000). Bax-dependent transport of cytochrome c reconstituted in pure liposomes. *Nature Cell Biol.* **2**, 553–555.
- Basanez, G., Zhang, J., Chau, N., Makshev, G. I., Frolov, V. A., Brandt, T. A. *et al.* (2001). Pro-apoptotic cleavage products of Bcl-x<sub>L</sub> form cytochrome c-conducting pores in pure lipid membranes. *J. Biol. Chem.* **276**, 31083–31091.
- Tsujimoto, Y. & Shimizu, S. (2000). VDAC regulation by the Bcl-2 family of proteins. *Cell Death Differ.* **7**, 1174–1181.
- Vander Heiden, M. G., Li, X. X., Gottleib, E., Hill, R. B., Thompson, C. B. & Colombini, M. (2001). Bcl-x<sub>L</sub> promotes the open configuration of the voltage-dependent anion channel and metabolite passage through the outer mitochondrial membrane. *J. Biol. Chem.* **276**, 19414–19419.
- Muchmore, S. W., Slatyer, M., Liang, H., Meadows, R. P., Harlan, J. E., Yoon, H. S. *et al.* (1996). X-ray and NMR structure of human Bcl-x<sub>L</sub>, an inhibitor of programmed cell death. *Nature*, **381**, 335–341.
- Fesik, S. W. (2000). Insights into programmed cell death through structural biology. *Cell*, **103**, 272–282.
- Matsuyama, S., Schendel, S. L., Xie, Z. & Reed, J. C. (1998). Cytoprotection by Bcl-2 requires the pore-forming  $\alpha 5$  and  $\alpha 6$  helices. *J. Biol. Chem.* **273**, 30995–31001.
- Minn, A. J., Vélez, P., Schendel, S. L., Liang, H., Muchmore, S. W., Fesik, S. W. *et al.* (1997). Bcl-x<sub>L</sub> forms an ion channel in synthetic lipid membranes. *Nature*, **385**, 353–357.
- Antonson, B., Conti, F., Ciavatta, A., Montesuit, S., Lewis, S., Martinou, I. *et al.* (1997). Inhibition of Bax channel-forming activity by Bcl-2. *Science*, **277**, 370–372.
- Schleisinger, P. H., Gross, A., Yin, X. M., Yamamoto, K., Saito, M., Waksman, G. & Korsmeyer, S. J. (1997). Comparison of the ion channel characteristics of proapoptotic Bax and antiapoptotic Bcl-2. *Proc. Natl Acad. Sci. USA*, **94**, 11357–11362.
- Kudla, G., Montesuit, S., Esques, R., Berrier, C., Martinou, J. C., Ghazi, A. & Antonsson, B. (2000). The destabilization of lipid membranes induced by the C-terminal fragment of caspase 8-cleaved Bid is inhibited by the N-terminal fragment. *J. Biol. Chem.* **275**, 22713–22718.
- Brockman, H. (1999). Lipid monolayers: why use half a membrane to characterize protein-membrane interactions? *Curr. Opin. Struct. Biol.* **9**, 438–443.
- Zhai, D., Miao, Q., Zin, X. & Yang, F. (2001). Leakage

<sup>†</sup> <http://geno3d-pbil.ibcp.fr>

- and aggregation of phospholipid vesicles induced by the BH3-only Bcl-2 family member, Bid. *Eur. J. Biochem.* **268**, 45–55.
24. Gillet, G., Guerin, M., Trembleau, A. & Brun, G. (1995). A BCL-2-related gene is activated in avian cells transformed by the *Rous sarcoma virus*. *EMBO J.* **14**, 1372–1381.
25. Lee, R. M., Gillet, G., Burnside, J., Thomas, S. J. & Neiman, P. (1999). Role of Nr-13 in regulation of programmed cell death in the bursa of Fabricius. *Genes Dev.* **13**, 718–728.
26. Moradi-Améli, M., Lorca, T., Ficheux, D., di Pietro, A. & Gillet, G. (2002). Interaction between the anti-apoptotic protein Nr-13 and cytochrome c. Antagonistic effect of the BH3 domain of Bax. *Biochemistry*, **27**, 8540–8550.
27. Lalle, P., Aoucheria, A., Dumont-Miscopein, A., Jambon, M., Venet, S., Bobichon, H. *et al.* (2002). Evidence for crucial electrostatic interactions between Bcl-2 homology domains BH3 and BH4 ion the anti-apoptotic Nr-13 protein. *Biochem. J.* **368**, 213–221.
28. Daum, G. (1985). Lipids of mitochondria. *Biochim. Biophys. Acta*, **822**, 1–42.
29. Krol, S., Ross, M., Sieber, M., Künneke, S., Galla, H. J. & Janshoff, A. (2000). Formation of three-dimensional protein-lipid aggregates in monolayer films induced by surfactant protein B. *Biophys. J.* **79**, 904–918.
30. Maggio, B. (1994). The surface behavior of glycosphingolipids in biomembranes: a new frontier of molecular ecology. *Prog. Biophys. Mol. Biol.* **62**, 55–117.
31. Marsh, D. (1996). Lateral pressure in membranes. *Biochim. Biophys. Acta*, **1286**, 183–223.
32. Schwarz, G. & Taylor, S. E. (1999). Polymorphism and interactions of a viral fusion peptide in a compressed lipid monolayer. *Biophys. J.* **76**, 3167–3175.
33. Wackerbauer, G., Weis, I. & Schwarz, G. (1996). Preferential partitioning of melittin into the air/water interface: structural and thermodynamic implications. *Biophys. J.* **71**, 1422–1427.
34. Losonczi, J. A., Olejniczak, E. T., Betz, S. F., Harlan, J. E., Mack, J. & Fesik, S. W. (2000). NMR studies of the anti-apoptotic protein Bcl-x<sub>L</sub> in micelles. *Biochemistry*, **39**, 11024–11033.
35. Russ, W. P. & Engelman, D. M. (2000). The GxxxG motif: a frame work for transmembrane helix-helix association. *J. Mol. Biol.* **296**, 911–919.
36. Falnes, P. & Sanvig, K. (2001). Penetration of protein toxins into cells. *Curr. Opin. Cell Biol.* **12**, 407–413.
37. Minn, A. J., Kettlun, C. S., Liang, H., Kelatar, A., Vander Heiden, M. G., Chang, B. S. *et al.* (1999). Bcl-xL regulates apoptosis by heterodimerization-dependent and -independent mechanisms. *EMBO J.* **18**, 632–643.
38. Nouraini, S., Six, E., Matsuyama, S., Krajewski, S. & Reed, J. C. (2000). The putative pore-forming domain of Bax regulates mitochondrial localization and interaction with Bcl-x<sub>L</sub>. *Mol. Cell Biol.* **20**, 1604–1615.
39. Shimizu, S. & Tsujimoto, Y. (2000). Proapoptotic BH3-only Bcl-2 family members induce cytochrome c release, but not mitochondrial membrane potential loss, and do not directly modulate voltage-dependent anion channel activity. *Proc. Natl Acad. Sci. USA*, **97**, 577–582.
40. Epand, R. F., Martinou, J. C., Fornaliez-Mulhauser, M., Hughes, D. W. & Epand, R. M. (2002). The apoptotic protein tBid promotes leakage by altering membrane curvature. *J. Biol. Chem.* **277**, 32632–32639.
41. Zamzami, N., El Hamel, C., Maise, C., Brenner, C., Munoz-Pinedo, C., Belzacq, A. S. *et al.* (2000). Bid acts on the permeability transition pore complex to induce apoptosis. *Oncogene*, **19**, 6342–6350.
42. Kuwana, T., Mackey, M. R., Perkins, G., Ellisman, M. H., Latterich, M., Schneider, R. *et al.* (2002). Bid, Bax, and lipids cooperate to form supramolecular opening in the outer mitochondrial membrane. *Cell*, **111**, 331–342.

Edited by M. Yaniv

(Received 21 May 2003; received in revised form 30 September 2003; accepted 8 October 2003)